Robust Algorithms for the Solution of the Ideal Adsorbed Solution Theory Equations

Enzo Mangano, Daniel Friedrich, and Stefano Brandani
Scottish Carbon Capture and Storage, Institute for Materials and Processes, School of Engineering,
The University Edinburgh, The King's Buildings, Mayfield Road, Edinburgh EH9 3JL, U.K.

The ideal adsorbed solution (IAS) theory has been shown to predict reliably multicomponent adsorption for both gas and liquid systems. There is a lack of understanding of the conditions which guarantee convergence for various algorithms used to solve the IAS theory equations and inconsistencies are present in the reported computational effort required for the different approaches. The original nested loop and the FastIAS technique are revisited. The resulting system of equations is highly nonlinear but both methods are shown to be robust if appropriate choices are made for the starting values of the unknown variables. New initial conditions are proposed and the resulting algorithms are compared in a consistent manner with the main methods available to solve the IAS theory equations. The algorithms are extended for the first time to all nontype I isotherms. © 2014 American Institute of Chemical Engineers *AIChE J*, 61: 981–991, 2015
Keywords: separations, thermodynamics, adsorption equilibria, ideal adsorbed solution theory, numerical algorithms

Introduction

The ideal adsorbed solution (IAS) theory of Myers and Prausnitz[1] has been shown to predict reliably multicomponent adsorption equilibrium for both gas and liquid systems. This is of major importance when modelling adsorption based separation processes, as the direct measurement of multicomponent isotherms is both challenging and very time consuming.[2] While clearly, not all adsorbed systems behave ideally, the solution of the IAS theory equations is also needed when extending the treatment to real adsorbed phases, as the IAS theory yields the reference state commonly used in the definition of the activity coefficients of the adsorbed mixtures.[3]

In the original contribution, Myers and Prausnitz[1] outlined the formulation of the problem, that is, derived the set of equations to be solved, but did not provide details of a solution algorithm as for binary systems it is possible to construct a graphical solution. Even though several algorithms are available to solve the multicomponent equilibrium problem[4–9] there appears to be a lack of understanding of the conditions which guarantee convergence to the physically correct solution. Furthermore, there are also inconsistencies in the reported computational effort required for the different approaches to solving the IAS theory equations. Part of the confusion stems from the fact that the various algorithms have often been developed based on specific isotherms and

the general characteristics of the problem have become somewhat difficult to understand. For example, the algorithms developed by Tien and coworkers[5,9] are in fact small variants of the general method of Myers and Valenzuela,[6] which we will call the nested loop algorithm. Because all the early algorithms have been developed for and applied to type I isotherms, there seems to be also no clarity on how to extend them to nontype I isotherms[4] and whether they are robust.

In this contribution, the nested loop method and the more advanced FastIAS technique are revisited and expressed in terms of general adsorption isotherms. The criteria for convergence of the algorithms are investigated in detail for type I isotherms. Both approaches are then extended for the first time to all nontype I isotherms.

Proof of Guaranteed Convergence of the Nested Loop Algorithm

The basic equations of the IAS are the analogue of Raoult's law in vapour–liquid equilibrium[1]

$$Py_i = P_i^0(\Pi)x_i \qquad i = 1, 2 \ldots Nc \qquad (1)$$

where P_i^0 is the pressure at which each pure component is at the same reduced spreading pressure, Π, and temperature of the mixture. The reduced or modified spreading pressure is defined by the Gibbs adsorption isotherm

$$\Pi = \frac{A\pi}{RT} = \Pi_i = \int_0^{P_i^0} \frac{q_i^0(P)}{P} dP \qquad i = 1, 2 \ldots Nc \qquad (2)$$

We note that this is the equivalent of the reduced grand potential of Myers and Monson.[3] Although, the reduced grand potential is a more appropriate name for this

thermodynamic variable in the remainder of this article, we will use the conventional and widely used term of reduced spreading pressure without loss of clarity. For liquid systems the same set of equations applies with pressure replaced by concentration.[10] For simplicity here we will refer always to pressure, with the understanding that all the results will apply to the corresponding liquid system. We note also that Eq. 2 implies the assumption of an ideal gas (for gases) or ideal liquid mixture (for liquids) and that fugacity should replace pressure in a rigorous extension to high-pressure gas systems or nonideal liquid mixtures, but this is beyond the scope of this contribution.

To close the problem, the total number of adsorbed moles can be found assuming zero area (equally for mass or volume[3]) change upon adsorption

$$\frac{1}{q_t} = \sum_{i=1}^{Nc} \frac{x_i}{q_i^0(P_i^0)} \qquad (3)$$

To calculate the equilibrium compositions one requires the knowledge of P_i^0 for all components. If the total pressure and gas phase composition are specified the simplest way to solve the problem is by a nested solution of nonlinear equations.[6] From Eq. 1 and the fact that the sum of the adsorbed phase mole fractions is unity we have

$$f(\Pi) = 1 - \sum_{i=1}^{Nc} \frac{Py_i}{P_i^0(\Pi)} = 0 \qquad (4)$$

Equation 4 is solved using Newton's method. Myers and Monson[3] point out that "Numerical solution of this equation is problematic because of its high degree of nonlinearity," but we will prove that an appropriate selection of the initial condition guarantees convergence. Before resolving this important issue, a point that is worth stating clearly is that while the calculation of the spreading pressure is made easier by the availability of an analytical expression for the integral in Eq. 2, in implementing Newton's method one needs the derivatives of the spreading pressure and these can be calculated directly for any isotherm from

$$\frac{d\Pi_i}{dP_i^0} = \frac{q_i^0(P_i^0)}{P_i^0} \qquad i = 1, 2 \ldots Nc \qquad (5)$$

and

$$\frac{df}{d\Pi} = \sum_{i=1}^{Nc} \frac{Py_i}{P_i^0 q_i^0(P_i^0)} \qquad (6)$$

In the formulation of this algorithm by Tien and coworkers[5,9] Eq. 2 is rewritten so that it can be solved by successive substitutions and the derivative of the spreading pressure is approximated from the resulting expression. In the formulation of the algorithm without approximations[6] an isotherm with an explicit expression for pressure as a function of spreading pressure, $P_i^0(\Pi)$, was used. In general this is not the case, so that at each iteration and for each component Eq. 2 has to be solved numerically using Newton's method.[11]

As the numerical solution of the nonlinear problem requires initial guesses for Π and P_i^0, one must ensure an appropriate selection to achieve a robust algorithm. This is seen as a key weakness of the original method and of the FastIAS algorithm.[4] To our knowledge, no formal proof of

convergence has been reported for the algorithm, so we proceed to demonstrate this and establish initial guesses that guarantee convergence.

The integrand in Eq. 2 is always positive, as both P and the number of moles adsorbed are positive and in the limit of zero P for any thermodynamically consistent adsorption isotherm the integrand will become the Henry law constant, K_i. This means that the spreading pressure increases monotonically as a function of pressure. Therefore for all type I isotherms $\Pi_i \in [0, \infty)$ and one must ensure that P_i^0 is nonnegative at each iteration. If we are solving in the inner loop

$$g_i(P_i^0) = \Pi_i^0 - \Pi = 0 \qquad i = 1, 2 \ldots Nc \qquad (7)$$

and

$$\frac{dg_i}{dP_i^0} = \frac{q_i^0}{P_i^0} \qquad i = 1, 2 \ldots Nc \qquad (7a)$$

$$\frac{d^2 g_i}{dP_i^{02}} = \frac{1}{P_i^0} \left(\frac{dq_i^0}{dP_i^0} - \frac{q_i^0}{P_i^0} \right) \qquad i = 1, 2 \ldots Nc \qquad (7b)$$

If the initial guess is in the region $[0, P_i^0(\Pi)]$, Eq 7 is negative and monotonically increasing. Newton's method is guaranteed to converge to a positive value if the second derivative is negative and does not change sign, that is, there are no inflection points.[12] For a type I isotherm the slope of the secant of the isotherm between 0 and P is always greater than the slope of the tangent in P, and therefore the second derivative, Eq. 7a, is always negative. One could choose 0 as the starting point, but in the limit of zero pressure

$$\Pi_i^0 = K_i P_i^0 \qquad i = 1, 2 \ldots Nc \qquad (8)$$

therefore, we can use

$$P_i^0 = \frac{\Pi}{K_i} \qquad i = 1, 2 \ldots Nc \qquad (9)$$

as this ensures that at the first iteration the value of g is negative for any type I isotherm.

We now turn to the analysis of Eq. 4. From the discussion above, it is also clear that all the $P_i^0(\Pi)$ are monotonic and increase with Π. As a result f is monotonic and it increases with Π. The second derivative is given by:

$$\frac{d^2 f}{d\Pi^2} = - \sum_{i=1}^{Nc} \frac{Py_i \left[\frac{q_i^0}{P_i^0} + \frac{dq_i^0}{dP_i^0} \right]}{q_i^{03}} \qquad (10)$$

As all the terms appearing in the summation are positive for any isotherm, there will be no inflection points—the second derivative is always negative—hence Newton's method is again guaranteed to converge to a positive value if we determine an initial guess that ensures that f is initially negative. For $\Pi = 0$ Eq. 4 yields $-\infty$ therefore, guaranteed convergence is ensured if one chooses any small initial value and this is true for any isotherm. More generally convergence is guaranteed for any value $(0, \Pi^*)$ as shown in Figure 1, where

$$\frac{df}{d\Pi}\bigg|_{\Pi^*} \Pi^* = f(\Pi^*) \qquad (11)$$

For initial values to the right of Π^* the first iteration of Newton's method would result in a negative spreading pressure for which the equations are obviously not defined.
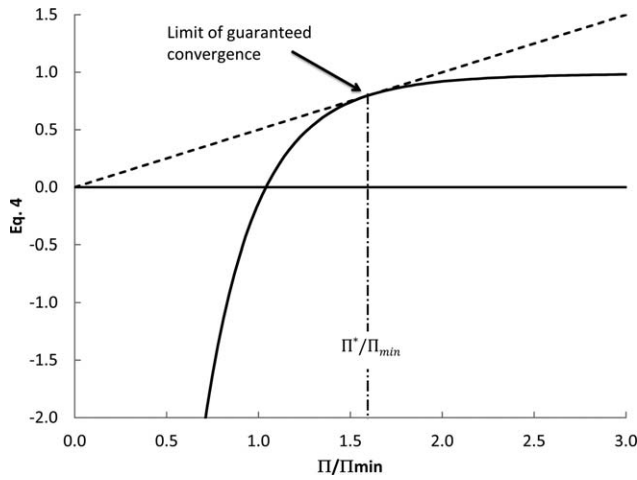
Figure 1. Qualitative shape of Eq. 4 and limit of guaranteed convergence.

Figure 2. Graphical construction in terms of reduced spreading pressure vs. KP.

We observe that choosing a very small initial value Π^0 will result in slow convergence. This can be seen by noting that in the Henry law limit it is possible to use the analytical expression for the spreading pressure and

$$P_i^0 = \frac{\Pi^0}{K_i} \qquad \text{at low spreading pressure} \qquad (12)$$

and combining this with Eq. 4

$$f\left(\Pi^0\right) = 1 - \frac{P}{\Pi^0} K_{\text{Ave}} \quad K_{\text{Ave}} = \sum_{i=1}^{Nc} y_i K_i \qquad (13)$$

and

$$\frac{df}{d\Pi}\bigg|_{\Pi^0} = \sum_{i=1}^{Nc} \frac{P y_i}{P_i^0(\Pi)^2} \frac{dP_i^0}{d\Pi} = \frac{PK_{\text{Ave}}}{\Pi^{02}} \qquad (14)$$

Therefore, at the next iteration

$$\Pi^1 = \Pi^0 \left(1 - \frac{\Pi^0 - PK_{\text{Ave}}}{PK_{\text{Ave}}}\right) < 2\ \Pi^0 \qquad (15)$$

This clearly shows that a smaller initial guess will give rise to a slower progression towards the solution. By the same argument one should avoid a starting point close to Π^* as at the second iteration one will be at a very small value of Π, as can be seen from Figure 1.

A better starting point, which still guarantees convergence, can be obtained using

$$\Pi^0 = \min\left[\Pi_i\left(\frac{PK_{\text{Ave}}}{K_i}\right)\right] \qquad (16)$$

or

$$\Pi^0 = \min[\Pi_i(P)] \qquad (17)$$

To prove that both Eqs. 16 and 17 are starting points that guarantee convergence, we simply note that from Eq. 1, summing over all components, we can obtain

$$P = \sum_{i=1}^{Nc} P_i^0(\Pi) x_i \qquad (18)$$
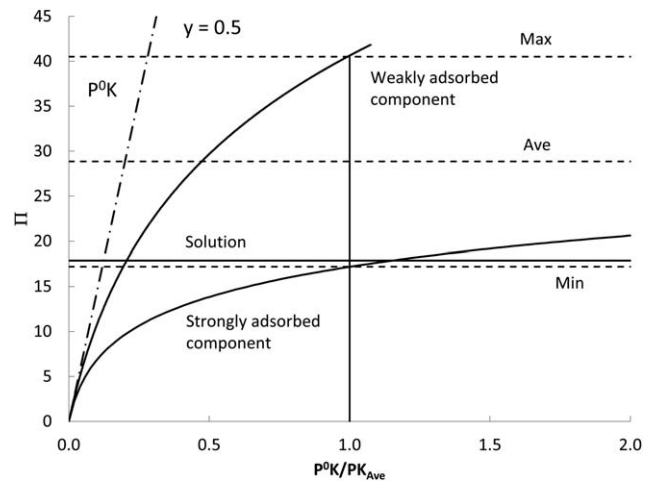
and similarly

$$PK_{Ave} = \sum_{i=1}^{Nc} P_i^0(\Pi) K_i x_i \qquad (19)$$

From Eq. 18 and 19, we can see that P is an average of all $P_i^0(\Pi)$ at the solution and PK_{Ave} is an average of all $P_i^0 K_i$. Figure 2 shows that in a plot of Π_i vs. $P_i^0 K_i$, PK_{Ave} will correspond to a vertical line that intercepts the various curves corresponding to the spreading pressures. In this plot, the solution that fulfils Eqs. 1 and 2 will be a horizontal line which cuts all the spreading pressure curves between the minimum and the maximum of all P_i^0, so within this range it will also cut the vertical line. The horizontal line must lie above at least one of the intersections of the vertical line due to the monotonicity of the spreading pressures. This proves the fact that at least one value of $P_i^0 K_i$ will be less than PK_{Ave}. In this plot the line $\Pi_i = P_i^0 K_i$ will be above all spreading pressures and as the pressure increases the difference between the various curves will increase. A similar approach can be applied to the plot of Π_i vs. P_i^0 and P will correspond to a vertical line which identifies Nc values of the spreading pressure. Similarly to the previous case, the minimum value will provide a starting point with guaranteed convergence. For a binary system, this plot is the one used for the graphical solution of the IAS equations presented by Myers and Prausnitz[1] and included in Figure 3.
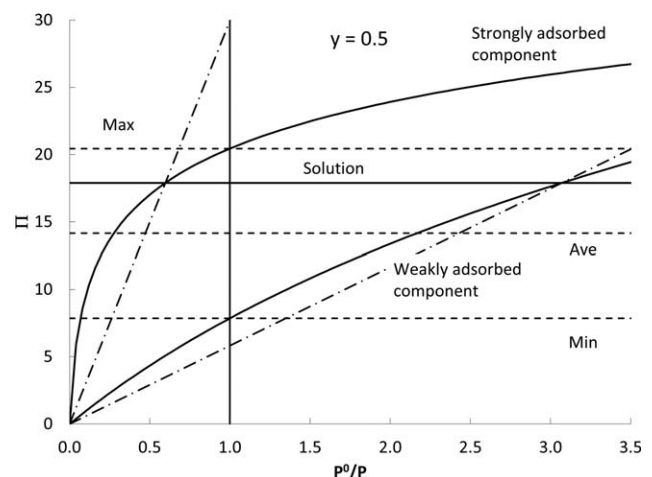

Figure 3. Graphical construction in terms of reduced spreading pressure vs. P.

Using the minimum value ensures that f is negative because the guess is lower than the solution and convergence to a positive value is guaranteed.

One can argue that the minimum obtained from $P_i^0 = \frac{PK_{Ave}}{K_i}$ is a better choice as this value corresponds to the exact solution in the limit of zero pressure and in general it is much closer to the solution. It is true though that by renormalizing all the curves so that they coincide at low pressure, there is an increase in the difference between the curves at high pressure. As we will see these considerations will be useful in the analysis of the robustness of the FastIAS algorithm where the current formulation will lead to a broader spread in the initial guesses of the spreading pressures. This is particularly true for the more weakly adsorbed component at high pressures.

Myers and Valenzuela[6] and Do[11] used as their initial guess

$$\Pi^0 = \sum_{i=1}^{Nc} y_i \Pi_i(P) \tag{20}$$

This initial guess does not guarantee convergence strictly, that is, f can be positive at the first iteration, but it reduces to the exact solution in the low-pressure limit (as for Eq. 16). This is simply due to the fact that in the low-pressure region the relationship between P_i^0 and Π is linear. Therefore, Eq. 20 can also be used but a check to ensure that Π remains positive at each iteration should be added to guarantee convergence. We also note that convergence may be slow when Π^0 is close to Π^*.

It is important to note that the discussion on the convergence of Eq. 4 relies only on the assumption that the adsorption isotherms of pure components increase monotonically, therefore, it is valid for any physically realistic isotherm. The nested loop algorithm for nontype I isotherms requires only a careful analysis of the convergence of Eq. 2.

The FastIAS Algorithm

O'Brien and Myers[7] introduced the FastIAS algorithm based on their adsorption isotherm[13] to improve the efficiency of the calculations for dynamic simulations of adsorption processes. They later reported[8] an improved revised algorithm and mentioned that it could be applied to any isotherm for which an analytical expression for the spreading pressure was available. The examples discussed in the article[8] were based on an earlier contribution[5] and focussed only on the O'Brien-Myers isotherm[13] and this may have left the reader with the impression that additional effort is required to derive the set of equations needed for other isotherms. For clarity, the FastIAS algorithm is outlined here without any mention to a specific isotherm.

The first step is to look at the isotherm equation and define a reduced pressure

$$\eta_i = Kp_i P_i^0 \quad i=1, 2 \ldots Nc \tag{21}$$

For Langmuir type isotherms the Kp_i are simply the ratio of the Henry law constant and the saturation capacity.

The IAS equations are then recast as a function of the dimensionless pressures and rather than solving Eqs. 2 and 4 as nested loops all the equations are solved simultaneously by defining the following system

$$Res_i = \Pi_i(\eta_i^0) - \Pi_{Nc}(\eta_{Nc}^0) \quad i=1,2 \ldots Nc-1$$
$$Res_{Nc} = 1 - \sum_{i=1}^{Nc} \frac{Kp_i Py_i}{\eta_i^0(\Pi)} \tag{22}$$

What makes the numerical solution particularly fast is the structure of the corresponding Jacobian, which has nonzero elements only on the diagonal, the last column and the last row. Therefore, the diagonal elements can be used to eliminate the elements of the last row and then all the solutions in the iteration are computed by back substitution from the resulting upper triangular matrix. The original algorithm of O'Brien and Myers[7] is similar but equates the spreading pressures of successive components. This results in a Jacobian that has nonzero elements on the diagonal, the elements just above the diagonal and the last row. In the original formulation, the algorithm did not use the structure of the matrix to improve the computational efficiency. If this is considered the number of computations is almost the same, there is only one extra multiplication and subtraction in the back-substitution step, when there are more than two components, that is, both versions are identical for a binary mixture. As the coding is slightly more complicated for the original formulation, we will only consider the improved 1988 version in what follows and refer to it for simplicity as the FastIAS algorithm. The reader should understand that the improvements by a factor of 4 in computational effort reported by O'Brien and Myers[8] for a 10 component system are almost exclusively due to the fact that the 1985 version used a dense matrix solver and the 1988 one explicitly used the sparse nature of the Jacobian.

Contrary to what is stated in O'Brien and Myers[8] the FastIAS algorithm can be used also when the residuals in Eq. 22 must be calculated by numerical integration as all the other terms needed are in analytical form. More generally if the nested loop algorithm is applicable, then the FastIAS is also applicable, a point not clearly stated in Landa et al.[4] The last row of the Jacobian of the system of Eq. 22 is given by

$$Jac_{Nc,i} = \frac{Kp_i Py_i}{\eta_i^0(\Pi)^2} \quad i=1,2 \ldots Nc \tag{23}$$

and the diagonal and last column elements of the Jacobian can be calculated directly from the isotherm. In fact there is no need to store the additional elements in the last column of the Jacobian as all the information can be stored in the following vector

$$Diag_i = \frac{q_i^0(\eta_i^0)}{\eta_i^0} \quad i=1,2 \ldots Nc \tag{24}$$

At any iteration of the Newton method the linear system being solved is

$$\overline{\overline{Jac}}\,\overline{\delta} = -\overline{Res} \tag{25}$$

Clearly in the elimination process only the last term in the last row of the Jacobian and the last element of the residual vector are modified

$$Jac_{Nc,Nc} = \frac{Kp_{Nc}Py_{Nc}}{\eta_{Nc}^0{}^2} + Diag_{Nc}\sum_{i=1}^{Nc-1} \frac{Jac_{Nc,i}}{Diag_i} \tag{26}$$

$$Res_{Nc} = 1 - \sum_{i=1}^{Nc} \frac{Kp_i Py_i}{\eta_i^0} - \sum_{i=1}^{Nc-1} \frac{Jac_{Nc,i}}{Diag_i} Res_i \tag{27}$$

The resulting system of equations with an upper triangular matrix can then be solved by direct back-substitution

$$\delta_{Nc} = -\frac{\text{Res}_{Nc}}{\text{Jac}_{Nc,Nc}} \qquad (28)$$

and

$$\delta_i = \frac{-\text{Res}_i + \text{Diag}_{Nc}\delta_{Nc}}{\text{Diag}_i} \quad i=1,2\ldots Nc-1 \qquad (29)$$

We note from Eqs 24 and 26 that all the diagonal elements of the resulting upper triangular matrix are positive and the system is never singular. Therefore there is always a direction in which the overall residual decreases and the FastIAS algorithm or a backtracking variant[14] will converge unless physically unrealistic (negative) values of the reduced pressures are obtained. This very important point shows that the FastIAS algorithm is intrinsically robust and appears to have been missed in previous studies.

The iteration is then repeated with a new set of dimensionless pressures until convergence

$$\eta_i^{\langle k+1 \rangle} = \eta_i^{\langle k \rangle} + \delta_i^{\langle k \rangle} \qquad i=1,2\ldots Nc \qquad (30)$$

Given that this is now the solution of a system of equations, to have a robust algorithm the initial set of reduced pressures has to be defined and a check has to be included so that all the dimensionless pressures remain positive at each iteration. This last point is the key to ensuring convergence and O'Brien and Myers[7,8] suggest to use

$$\eta_i^{\langle k+1 \rangle} = \frac{\eta_i^{\langle k \rangle}}{2} \quad \text{if} \quad \eta_i^{\langle k \rangle} + \delta_i^{\langle k \rangle} < 0 \qquad (31)$$

along with the following set of initial guesses

$$\eta_i^{\langle 0 \rangle} = \frac{Kp_i}{K_i}PK_{\text{Ave}} \qquad (32)$$

The use of Eq. 31 does ensure convergence, but can reduce the order of convergence. In most cases it is invoked at the first iteration, rarely at the second and higher iterations, normally for the more weakly adsorbed component and further away from the linear low-pressure limit. This can be understood with reference to Figure 2, as the spreading pressure calculated from the initial guess in Eq. 32 will be much higher than the solution and as a result the calculated step tends to move η to a negative value. Under certain conditions, Eq. 31 is not invoked as the calculated η remains positive but becomes very small. If this happens then qualitatively, for the same reasons for which convergence is slow for the nested loop algorithm, an increased number of iterations are needed to arrive at the solution. Having understood the criteria for rapid convergence of the nested-loop algorithm, it is therefore, possible to identify an improved set of initial conditions valid when the pressure is high

$$\eta_i^{\langle 0 \rangle} = \min\left(\frac{Kp_i}{K_i}PK_{\text{Ave}};PKp_i\right) \qquad (33)$$

While this condition does not guarantee strict convergence it resolves the issue related to the more weakly adsorbed component, that is, avoids extrapolation to high spreading pressures, and combined with Eq. 31 results in an algorithm that is both robust and more efficient than the original FastIAS approach at high pressures.

A step by step example of the solution of a ternary equilibrium systems for both the nested loop and FastIAS algorithms is included in the Supporting Information.

The Algorithm of Landa et al.[4]

An alternative approach to solving the IAS theory equations has been presented recently by Landa et al.[4] This method is based on converting the following equation

$$\Pi_1\left(P_1^0\right) = \Pi_i\left(P_i^0\right) \rightarrow \frac{d\Pi_1\left(P_1^0\right)}{dP_1^0} = \frac{d\Pi_i\left(P_i^0\right)}{dP_i^0}\frac{dP_i^0}{dP_1^0} \quad i=1,2\ldots Nc \qquad (34)$$

into a nonautonomous initial value (NAIV-IAS) problem, that is, the integration of a system of ordinary differential equations (ODEs)

$$\frac{dP_i^0}{dP_1^0} = \frac{q_1^0\left(P_1^0\right)}{P_1^0}\frac{P_i^0}{q_i^0\left(P_i^0\right)} \quad P_i^0(0)=0 \quad i=1,2\ldots Nc \qquad (35)$$

recognizing that Eq. 34 corresponds to fixed trajectories for all pure component pressures (or concentrations) that fulfil the condition that the spreading pressures remain the same. Clearly

$$\frac{dP_1^0}{dP_1^0} = 1 \qquad (36)$$

The integration of the system of ODEs stops when the equilibrium condition given by Eq. 4 is achieved. The great advantage of this algorithm is its simplicity and robustness. The fact that it requires only the computation of the adsorption isotherm means that it is applicable to any isotherm, but for type II and type III isotherms a check needs to be included to guarantee that a feasible solution is possible. We will return to this point when we discuss the extension of the nested loop and FastIAS algorithms to nontype I isotherms.

When this approach was presented, a comparison of the computational effort with respect to the FastIAS algorithm and the original nested loop approach was included. The conclusion[4] reached was that the NAIV-IAS algorithm was computationally comparable to the nested-loop algorithm and the FastIAS algorithm was approximately 20 times faster. O'Brien and Myers[7] compared their algorithm to the original algorithm of Myers and Prausnitz[1] and concluded that they improved the calculations by a factor of 25, but they did not clarify what starting values they used for the original method thus making it impossible to check their comparison. Moon and Tien[5] showed that their approach was in fact faster than the O'Brien and Myers[7] FastIAS method by a factor of 3–4. This led O'Brien and Myers to produce the improved FastIAS algorithm which was optimized for multicomponent systems to take into account the structure of the Jacobian and was shown to be up to 2 times faster than the Moon and Tien[5] method, which is a variant of the nested loop algorithm. There seems to be some confusion over the comparison of the computational speeds for the different algorithms and we will therefore address also this issue in detail.

Considering that the solution of the ODE system in the NAIV-IAS approach corresponds to applying quadrature formulae to the integral that gives the spreading pressure (in fact the ratio of the integrands) and that the net gain is to reduce by one the number of integrals that need to be carried out, it would seem more likely that the nested loop should still be faster when an analytical expression for the spreading pressure is available, especially with a large number of
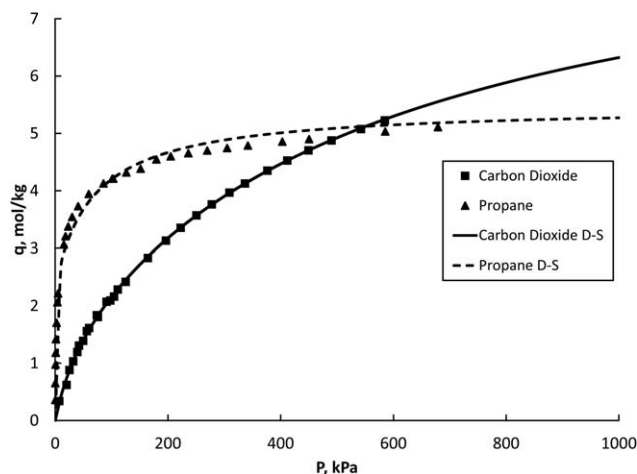
Figure 4. Experimental isotherms for CO₂ and propane and analytical isotherms fitted using the dual site Langmuir model.

components. In the section that follows we present a detailed comparison of the three algorithms, initially for a binary system, which allows a more in depth understanding of the issues which may slow down the convergence, and then for a 10 component system originally considered by Moon and Tien.[5]

Results for Type I Isotherms

As a test system, we consider the binary adsorption for CO_2–propane on NUXIT-AL activated carbon.[15,16] The isotherms of the pure components are shown in Figure 4 along with the analytical isotherms fitted to the experimental data (parameters are listed in Table 1). This binary pair is an interesting test system as it is not possible to regress accurately the pure component data using the thermodynamically consistent equal saturation capacities in the multisite Langmuir model.[17–19] This implies that a generalized Langmuir isotherm for this system is not thermodynamically consistent and the only way to predict binary adsorption equilibria reliably is through the IAS theory. The system also shows a case where the spreading pressures cross at high loadings, that is, where selectivity reversal is present.

To compare the execution times of the actual algorithm and not the time associated with the initialization of the code a loop is repeated 100 times for each calculation and the minimum time recorded was used as an indication of the actual execution time. This is an important aspect which when comparing the relative performance of the algorithms should eliminate any uncertainty associated with the choice of compiler or simulation environment and actual computer and may explain some of the results reported recently.[4] With this regard we also note that, in writing the code for the nested loop and the FastIAS the expression of the isotherm and the spreading pressure can be either written as part of

the main code or as an external function which is then called during the execution of the main code. Clearly, the second solution allows to have a more flexible code which can be used for different isotherms without the need to modify the main part of the code. On the other hand this makes the execution of the code in Matlab slower. Generally, we have noted that calling external functions for the isotherm and the spreading pressure makes the execution of the code about 2–3 times slower than having the isotherm and spreading pressure "embedded" in the main section. Figure 5 compares the execution times for the case in which the code is optimised for speed and the case in which external functions for the isotherm and the spreading pressure are used. In this example a dual-site isotherm is used and the molar fraction is varied from 0.01 to 0.99 at a total pressure of 1000 kPa.

The implementation of the NAIV-IAS method in Matlab requires a code structure in which the main code calls an external function for the ODE solver. For this reason it was decided that for the purpose of the comparison of the different methods external function calls would be used for all algorithms.

To explore a wide range of initial conditions three different cases have been considered. The first is to span the gas phase molar fraction from $y_1 = 0.01$ to 0.99 to look at mixtures in the transition from being rich in the more strongly adsorbed component to being rich in the more weakly adsorbed component. This is performed at three pressures 10, 100 and 1000 kPa, which correspond to low, intermediate and high-pressure conditions where the isotherms are close to linear, in the transition region for the more weakly adsorbed component and nonlinear for both components, respectively.

The second is to consider a single composition and span pressure, that is, similar to a pressurization step in a pressure swing adsorption simulator, to see the effect of increasing nonlinearity on execution times.

The third is to consider the case where the concentration sweep, $y_1 = 0.01$ to 0.99 at 0.01 intervals, is replicated, but the solution from the previous step is used as the initial guess. This example is used to test the algorithms in a case

Table 1. Dual Site Langmuir Isotherm Parameters

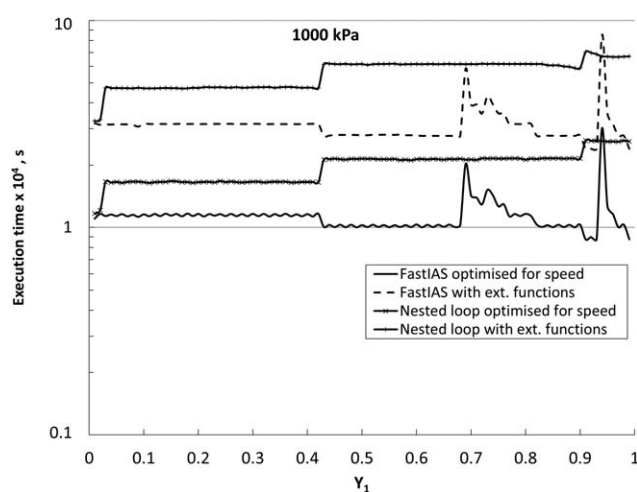| Component	CO₂	Propane
qs_1 [mol/kg]	1.46836	2.58
b_1 [1/kPa]	0.0244	0.95254
qs_2 [mol/kg]	7.89083	2.9
b_2 [1/kPa]	0.00165	0.01316

Figure 5. Comparison of the execution time for the FastIAS and nested loop codes in the case in which codes are optimised for speed and when external functions for isotherm and spreading pressure are used.
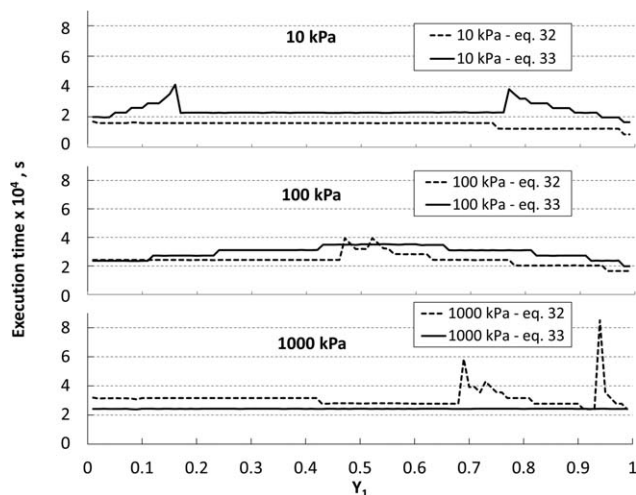
Figure 6. Execution times for the FastIAS method at different total pressures for different initial guesses.

Figure 8. Execution times for the nested loop method at different total pressures, using as initial guess Eqs. 20 and 16.

similar to where one uses the IAS theory in a dynamic adsorption column simulator. In this case, the comparisons of the execution times given by the previous two cases are only valid if the initial guess does not use the values at the previous time step. The requirement to adopt an even faster solution algorithm becomes increasingly important if the adsorption simulations are to be coupled with optimization tools.

Figure 6 shows the execution time as function of the mole fraction of CO_2, y_1, for the original FastIAS and the new approach proposed here. Clearly, both methods show very similar execution times at the different pressures, with the O'Brien method being slightly faster at the low and intermediate pressures and the new method being faster at the higher pressure. The execution time for the two methods is strictly related to the number of iterations required. Figure 7 shows the number of iterations required for each composition along with a flag that identifies if Eq. 31 is invoked. The flag is set to 0 if Eq. 31 is not used; 1 if it is invoked for component 1; 2 if it is invoked for component 2; and 3 if it is invoked for both components. From the plot it can be seen that when
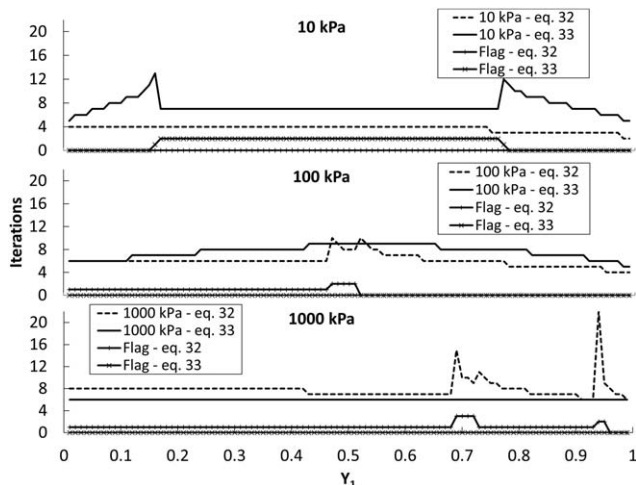
using the initial guess strategy proposed here Eq. 31 is never invoked at 100 and 1000 kPa.

Figure 8 shows a similar comparison for the nested loop algorithm with the different initial conditions, Eqs. 16 and 20. As it can be seen from the plot, the new initial strategy proposed using Eq. 16 improves the performance of the original nested loop under all conditions. The improvement in the total execution time with the proposed new method is approximately 38, 36, and 19% at 10, 100 and 1000 kPa, respectively.

Figure 9 shows the ratio of the execution times of the nested loop (initial guess Eq. 16) and NAIV-IAS algorithms compared to the FastIAS approach at different pressures. From the plot it can be seen that the new nested loop approach is 2–3 times slower than the FastIAS algorithm, while the NAIV-IAS method is about 20–30 times slower than the FastIAS at all the pressures.

Figure 10 shows the comparison of the execution times for the FastIAS, with the two initial guess strategies, the nested loop and the NAIV-IAS methods. In this case, the gas phase concentration is kept constant ($y_1 = 0.5$) while the total

Figure 7. Total number of iteration for FastIAS at different pressures using Eq. 32 and Eq. 33.

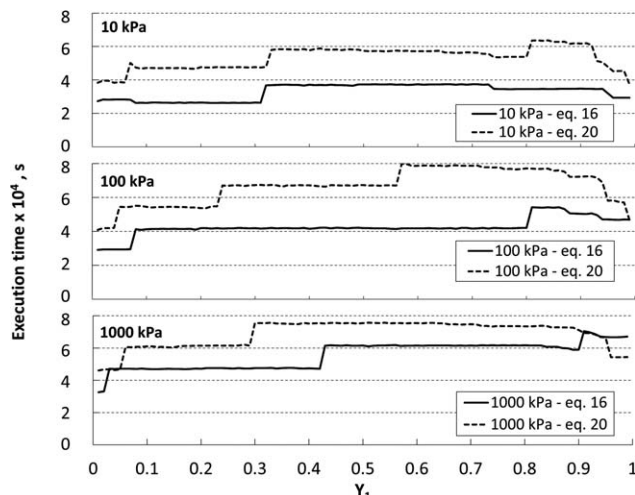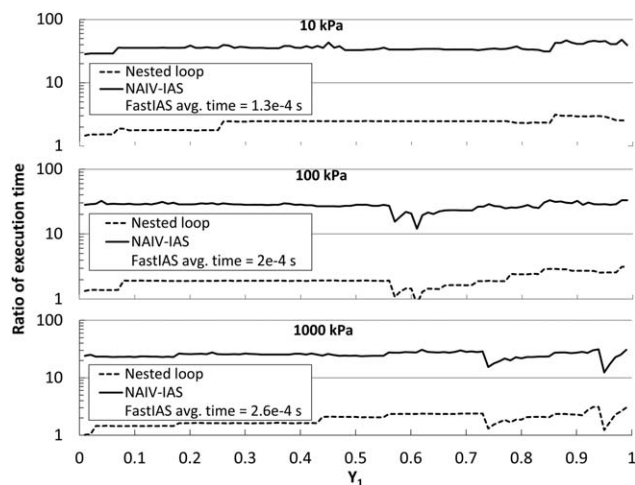Flags indicating when Eq. 31 is invoked are also shown for both methods.

Figure 9. Ratio of execution times for the nested loop and the NAIV-IAS method compared to FastIAS (actual execution times are reported in the Supporting Information).
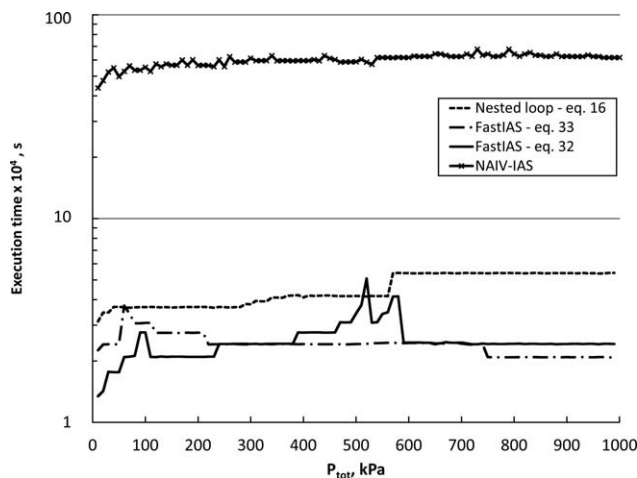
Figure 10. Execution times for the FastIAS, nested loop, and NAIV-IAS algorithms at $y_1 = 0.5$ and different total pressures.

pressure is increased from 10 to 1000 kPa. The plot shows how in the case of the FastIAS the algorithm may be further optimised by creating a routine that choses which initial guess strategy to use depending on the pressure range.

Figure 11 shows the ratio of the execution times for the three algorithms compared to the FastIAS algorithm as a function of mole fraction (the average execution for the FastIAS is included in the legend), when the initial guess is taken from the previous step. The nested loop and the FastIAS algorithms, which are based on Newton methods, clearly improve their performance relative to the NAIV-IAS approach, becoming 50–100 times faster. This is due to the quadratic convergence rate when the initial guess is close to the solution. Clearly, an adsorption process simulator can be optimised to reduce execution time by adding a step which stores the solutions to the IAS theory equations when using the FastIAS of nested loop methods.
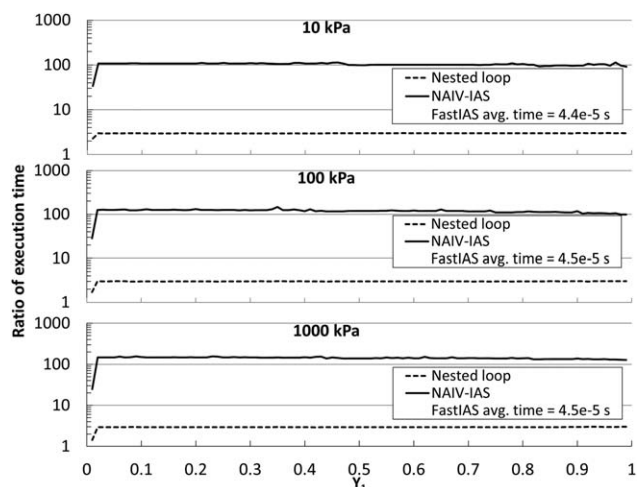

Figure 11. Ratio of the execution times for the FastIAS, the nested loop and the NAIV-IAS algorithms at different pressure in the case in which the solution from the previous step is used as initial guess (actual execution times are reported in the Supporting Information).

Table 2. Parameters for the O'Brien and Myers Isotherm for the 10 Components Problem[4,8]

Component, i	q_i^{sat} (mol/kg)	b_i (kPa^{-1})	σ_i (–)	y_i
1	5	0.01	1.2	0.1
2	3	0.006	1.1	0.01
3	4	0.0009	0.8	0.01
4	2	0.01	1.2	0.05
5	3.5	0.005	1	0.2
6	4	0.001	1.1	0.2
7	2	0.015	1.2	0.1
8	2.5	0.001	1.15	0.2
9	4	0.0001	1	0.02
10	5.5	0.006	1	0.11

All the cases considered confirm that the FastIAS algorithm is to be considered the state-of-the-art approach, with the nested loop being a reasonably close second.

As a final comparison we also considered the 10 component problem which, according to O'Brien and Myers,[8] fails to converge using the algorithm from Moon and Tien[5] at the conditions specified in Table 2. As expected there are no convergence issues with the nested loop algorithm and the ratio of the execution times are in line with the results obtained for the binary systems as shown in Table 3.

Applying the FastIAS and Nested Loop Algorithms to NonType I Isotherms

For the FastIAS algorithm, no special issues arise for nontype I isotherms with the exception of those isotherms which are not defined above a maximum allowable pressure (i.e., where condensation occurs – type II and III[18]). It is not difficult to resolve this problem as one has to include a check so that the reduced pressure remains within the physically valid limits, including the initial guesses. This can be expressed as

$$\eta_i^{\langle k+1 \rangle} = \eta_i^{\langle k \rangle} + \frac{\eta_i^{\max} - \eta_i^{\langle k \rangle}}{2} \quad \text{if } \eta_i^{\langle k \rangle} + \delta_i^{\langle k \rangle} > \eta_i^{\max} \quad (37)$$

It is important to note that for type II and III isotherms there is also an upper limit on the pressure that can be set for the mixture. In the case that all components have a maximum allowable pressure, from Eq. 1

$$\frac{1}{P_{\text{tot}}^{\max}} = \sum_i \frac{y_i}{P_i^{\max}} \quad (38)$$

This is an intrinsic requirement of the IAS theory and therefore applies to all algorithms. In the nested loop algorithm attention is needed for the numerical solution of the inversion of the spreading pressure equation. Clearly, if an analytical expression is available for $P_i^0(\Pi)$ then there are no issues to consider as is the case for the anti-Langmuir isotherm (type III). In the general case though, from Eq. 7b, one has to identify the point(s) P^* where

$$\frac{dq_i^0}{dP_i^0} = \frac{q_i^0}{P_i^0} \quad (39)$$

which can be found easily by looking at the isotherm for each pure component. Convergence is guaranteed if the

Table 3. Execution Times for the 10 Component Case at $P = 300$ kPa

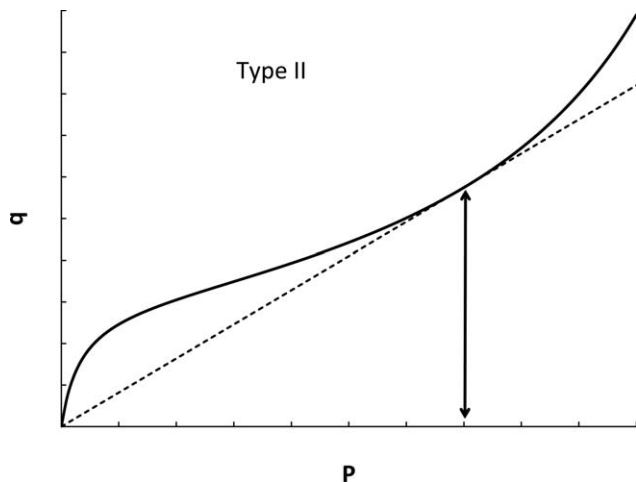| Nested loop	FastIAS	NAIV-IAS
2.2×10^{-3} s	5.6×10^{-4} s	6.2×10^{-3} s

Figure 12. Graphical solution of Eq. 39 for a Type II isotherm.

initial guess gives a value that has the same sign as the second derivative.

We will outline the solution for a specific isotherm that belongs to each category of isotherms. When solving the IAS theory equations for type II isotherms, we consider here a Brunauer–Emmett–Teller (BET) isotherm,[20] there will be only one inflection point in the spreading pressure. This can be identified easily as shown in Figure 12 and given the pure component parameters all P_i^* can be defined before the numerical solution of the IAS theory equations. For a BET isotherm

$$q_i(P_i^0)=q_{Si}\frac{a_iP_i^0}{(1-b_iP_i^0)(1-b_iP_i^0+a_iP_i^0)} \quad (40)$$

it is possible to derive the analytical solution and

$$P_i^*=\frac{a_i-2b_i}{2a_ib_i-2b_i^2} \quad (41)$$

Clearly for the BET isotherm

$$P_i^{\max}=\frac{1}{b_i} \quad (42)$$

If $P_i^0 < P_i^*$ the same criteria for convergence as discussed for type I isotherms apply, while for $P_i^0 > P_i^*$ Newton's method will converge if the initial guess corresponds to a value of $g_i(P_i^0) > 0$. A simple search will suffice as one can start with

$$P_i^0=\frac{P_i^*+P_i^{\max}}{2} \quad (43)$$

and if needed continue to halve the interval between P_i^0 and $P_i^{\max}$ until the function becomes positive.

For type III isotherms $P_i^*=0$ and the same approach used for type II isotherms above the inflection point will guarantee convergence.

When a quadratic isotherm is used[4,21]

$$q_i(P_i^0)=q_{Si}\frac{a_iP_i^0+2b_iP_i^{02}}{1+a_iP_i^0+b_iP_i^{02}} \quad (44)$$

if all the coefficients are positive, it is possible to obtain either type I or type V isotherms. For type V isotherms we have again only one inflection point in the spreading pres-

sure and Figure 13 shows how to identify it directly on the plot of the isotherm.

For the quadratic isotherm we can also find the analytical solution for Eq. 39

$$P_i^*=\frac{-a_i+\sqrt{4b_i-a_i^2}}{2b_i} \quad (45)$$

If all the coefficients in the isotherm are positive, from this equation it is clear that the inflection point is present if $a_i^2 < 2b_i$.

If the spreading pressure is below the inflection point, the same approach as for type III isotherms applies. If we are above the inflection point, then one needs to search for an initial value so that $g_i(P_i^0) < 0$. One can simply start at double the inflection point pressure and if needed halve the interval between the guess and the inflection point until a negative value of the function is found.

For type IV isotherms there will be two points where Eq. 39 is fulfilled, P_{1i}^* and P_{2i}^*, which again can be identified before solving the IAS theory equations. This is shown in Figure 14. A type IV isotherm can be obtained from a quadratic plus Langmuir isotherm with certain ranges of the isotherm parameters

$$q_i(P_i^0)=q_{S1i}\frac{a_iP_i^0+2b_iP_i^{02}}{1+a_iP_i^0+b_iP_i^{02}}+q_{S2i}\frac{c_iP_i^0}{1+c_iP_i^0} \quad (46)$$

The analytical solution for Eq. 39 is in the form of a quartic polynomial

$$P_i^{*4}+AP_i^{*3}+BP_i^{*2}+CP_i^*+D=0 \quad (47)$$

where

$$A=\frac{2a_ib_ic_i^2(q_{S1i}+q_{S2i})+4b_i^2c_iq_{S1i}}{b_i^2c_i^2(2q_{S1i}+q_{S2i})};$$

$$B=\frac{2b_ic_i^2(q_{S2i}-q_{S1i})+4a_ib_ic_iq_{Si}+a_i^2c_i^2q_{S2i}+2b_i^2q_{S1i}}{b_i^2c_i^2(2q_{S1i}+q_{S2i})}$$

$$C=\frac{2a_ic_i^2q_{S2i}+2a_i^2c_iq_{S1i}+2a_ib_iq_{S1i}-4b_ic_iq_{S1i}}{b_i^2c_i^2(2q_{S1i}+q_{S2i})};$$

$$D=\frac{a_i^2q_{S1i}+c_i^2q_{S2i}-2b_iq_{S1i}}{b_i^2c_i^2(2q_{S1i}+q_{S2i})}$$
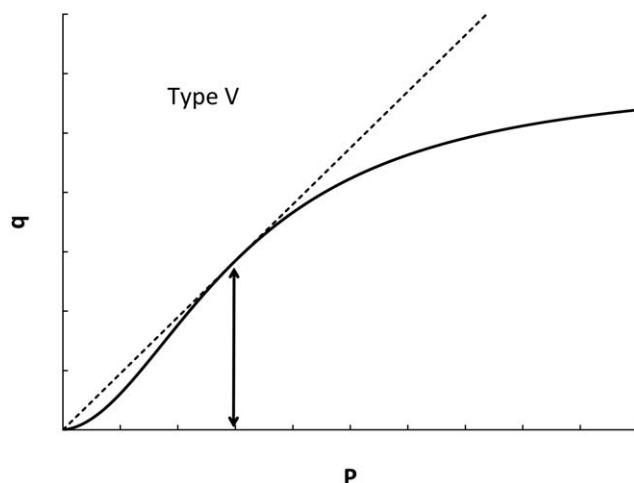

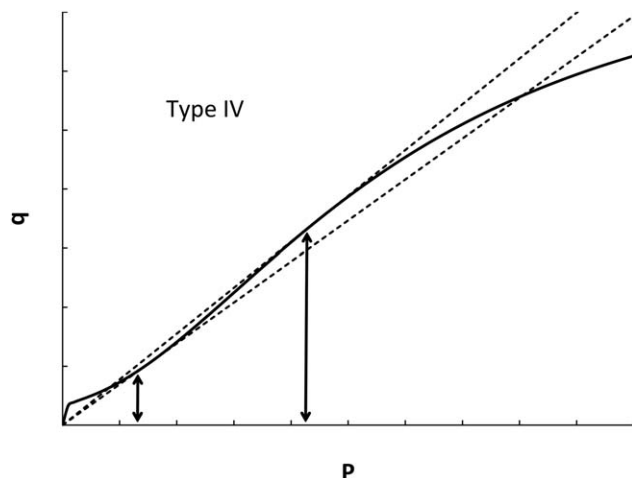**Figure 13. Graphical solution of Eq. 39 for a Type V isotherm.**

Figure 14. Graphical solution of Eq. 39 for a Type IV isotherm.

From the sign of the coefficients of the polynomial it is possible to find the number of positive roots (based on the number of sign changes[22] there can be no roots = type I isotherm; one root = type V isotherm; two roots = type IV isotherm). For two roots it is necessary for B to be negative, hence a high c_i combined with $q_{S1i} > q_{S2i}$ is required. A solid with a small amount of micropores and a large surface, which behaves as a type V isotherm, will yield a type IV overall isotherm. In this case there are two inflection points, $P^*_{1i} < P^*_{2i}$. For $P^0_i < P^*_{1i}$ the system will be the same as for a type I isotherm, while for $P^0_i > P^*_{2i}$ we are in the same case as for a type V isotherm above the inflection point. In the intermediate region one can initiate the search for a positive initial value starting with the mean and then iterate by halving the interval between the initial guess and P^*_{2i} until the value of g_i is positive.

From the discussion in this section it should be clear that it is always possible to construct a robust algorithm for both the FastIAS and the nested loop approaches which guarantees convergence for any isotherm. As this is achieved by preprocessing, that is, analysing the shape of the isotherms before any calculation, the actual simulation times will be close to those of the simpler type I isotherms. The Supporting Information includes examples for the nontype I isotherms along with a detailed comparison of the simulation times, confirming that the general trends observed for type I isotherms are still valid. Given the significant difference in computational speeds with other algorithms, it is clearly worth the small additional effort especially if one has to simulate complex adsorption processes which may be embedded in an optimization scheme.

Conclusions

General robust algorithms have been developed for the solution of the IAS theory equations for any type of adsorption isotherm. A formal proof of convergence has been derived for the first time to demonstrate that the nested loop algorithm is guaranteed to converge provided that the initial guess for the equation used to solve for the spreading pressure yields a negative value for the function for any type of adsorption isotherm. A new starting point,

consistent with the correct low-pressure limit, results in a procedure that is on average twice as fast as the original approach of Myers and Valenzuela[6] at higher pressures and has the further advantage of fulfilling the strict convergence criteria.

The FastIAS algorithm has been reformulated in terms of a generic isotherm and has been shown to yield a Jacobian that is always positive definite for any type of adsorption isotherm. As a result either the original algorithm or a backtracking variant are guaranteed to converge and the only remaining issue that is easily dealt with is linked with having to impose additional conditions that ensure that the calculated pressures remain within the physically valid limits.

The original nested loop and the FastIAS algorithms have been successfully extended to all nontype I adsorption isotherms. A simple procedure that requires preprocessing of the isotherm allows the selection of the conditions in which the nested loop algorithm is guaranteed to converge and the application has been demonstrated for type II–V isotherms.

A detailed comparison of computational times for the different algorithms considered indicates that the FastIAS algorithm is the state-of-the-art approach to solving the IAS theory equations. The nested loop algorithm is up to 2–3 times slower and the recent NAIV-IAS algorithm is typically 10–20 times slower for all cases considered in Matlab.

Literature Cited

1. Myers AL, Prausnitz JM. Thermodynamics of mixed-gas adsorption. *AIChE J*. 1965;11(1):121–127.
2. Sircar S. Basic research needs for design of adsorptive gas separation processes. *Ind Eng Chem Res*. 2006;45(16):5435–5448.
3. Myers A, Monson P. Physical adsorption of gases: the case for absolute adsorption as the basis for thermodynamic analysis. *Adsorption*. 2014;20(4):591–622.
4. Landa HOR, Flockerzi D, Seidel-Morgenstern A. A method for efficiently solving the IAST equations with an application to adsorber dynamics. *AIChE J*. 2013;59(4):1263–1277.
5. Moon H, Tien C. Further work on multicomponent adsorption equilibria calculations based on the ideal adsorbed solution theory. *Ind Eng Chem Res*. 1987;26(10):2042–2047.
6. Myers AL, Valenzuela D. Computer algorithm and graphical method for calculating adsorption equilibria of gas mixtures. *J Chem Eng Japan*. 1986;19(5):392–396.
7. O'Brien JA, Myers AL. Rapid calculations of multicomponent adsorption equilibria from pure isotherm data. *Ind Eng Chem Process Des Dev*. 1985;24(4):1188–1191.
8. O'Brien JA, Myers AL. A comprehensive technique for equilibrium calculations in adsorbed mixtures: the generalized FastIAS method. *Ind Eng Chem Res*. 1988;27(11):2085–2092.
9. Wang S-C, Tien C. Further work on multicomponent liquid phase adsorption in fixed beds. *AIChE J*. 1982;28(4):565–573.
10. Radke CJ, Prausnitz JM. Thermodynamics of multi-solute adsorption from dilute liquid solutions. *AIChE J*. 1972;18(4):761–768.
11. Do DD. *Adsorption Analysis: Equilibria and Kinetics*. London: Imperial College Press, 1998.
12. Morris JL. *Computational Methods in Elementary Numerical Analysis*. New York: Wiley, 1983.
13. O'Brien JA, Myers AL. Physical adsorption of gases on heterogeneous surfaces. Series expansion of isotherms using central moments of the adsorption energy distribution. *J Chem Soc Faraday Trans 1: Phys Chem Condens Phases*. 1984;80(6):1467–1477.

14. Press WH, Teukolsky SA, Vetterling WT, Flannery BP. *Numerical Recipes in C: The Art of Scientific Computing*. 3rd ed. Cambridge: Cambridge University Press, 2007.

15. Szepezy L, Illes V. Adsorption of gases and gas mixtures. Measurement of adsorption isotherms of gases on active carbon up to pressures of 1000 Torr. *Acta Chim Acad Sci Hung*. 1962;35(1):37–53.

16. Valenzuela D, Myers AL. Gas Adsorption Equilibria. *Sep Purif Rev*. 1984;13(2):153–183.

17. Rao MB, Sircar S. Thermodynamic consistency for binary gas adsorption equilibria. *Langmuir*. 1999;15(21):7258–7267.

18. Ruthven DM. *Principles of Adsorption and Adsorption Processes*. New York: Wiley, 1984.

19. Young DM, Crowell AD. *Physical adsorption of gases*. Washington, D.C.: Butterworths; 1962.

20. Tarafder A, Mazzotti M. A method for deriving explicit binary isotherms obeying the ideal adsorbed solution theory. *Chem Eng Technol*. 2012;35(1):102–108.

21. Guiochon G, Shirazi SG, Katti AM. *Fundamentals of Preparative and Nonlinear Chromatography*. Boston: Academic Press, 1994.

22. Green D, Perry R. *Perry's Chemical Engineers' Handbook*, Eighth Edition. New York: McGraw-Hill Education, 2007.